POLYMERS FOR SURFACE-FUNCTIONALIZATION AND BIOCOMPATIBILITY OF INORGANIC NANOCRYSTALS

Introduction

Inorganic nanocrystals such as those made of semiconductors (quantum dots, QDs), metals, and metal oxides are greatly promising for numerous applications ranging from developing optical and electronic devices to sensing and cellular imaging (1–4). They exhibit an array of unique physical, optical and chemical properties. They also present a series of challenging fundamental problems to investigate and understand. Some of these unique features include (1) size- and composition-tunable absorption and photoluminescence properties, high brightness combined with a remarkable photo- and chemical stability exhibited by QDs (5); (2) size- and shape-dependent surface plasmon resonance band for gold and silver nanoparticles (AuNPs and AgNPs) (6); and (3) strong size- and composition-dependent coercivity exhibited by iron oxide and other transition metal nanoparticles (eg, nanoparticles made of Fe_3O_4, Mn-doped Fe_3O_4, Pt, Ni, and Co) (7–10). These features combined have generated a tremendous interest and activity in the past decade (11–15). One of the much explored applications is geared toward the use of these materials as platforms for biological sensing and imaging, and as diagnostic tools.

Several methods have been reported to grow such nanocrystals directly in aqueous media (16,17). For instance, one of the simplest methods to prepare water soluble QDs, including CdTe, CdSe, and CdS, is arrested precipitation in the presence of stabilizer molecules, which provides nanocrystals that are capped with small thioalkyl acids (eg, thioglycolic acid, TGA, or mercaptopropionic acid, MPA) (17). However, this route tends to provide nanocrystals with rather large size dispersity and limited colloidal stability in buffer media with varying pHs and in the presence of added electrolytes and/or reducing agents. In addition, this route does not consistently allow easy and straightforward functionalization of the nanoparticle surfaces necessary for further coupling to the biological molecules (18).

To date, the highest quality nanocrystals with good control over the size, morphology, and crystallinity along with low size dispersity are mostly synthesized using reduction of organometallic precursors at high temperature and in the presence of hydrophobic coordinating molecules (ligands) (19–22). Commonly used ligands include trioctyl-phosphine (TOP), trioctyl-phosphine oxide (TOPO), alkylamine and alkylcarboxy for luminescent QDs, didodecyldimethylammonium

Encyclopedia of Polymer Science and Technology. Copyright © 2013 John Wiley & Sons, Inc. All rights reserved.

bromide for AuNPs, and oleic acid for iron oxide nanoparticles. However, this high temperature route tends to provide colloidal nanocrystals capped with hydrophobic ligands that are only dispersible in organic solvents, albeit with great long-term colloidal stability and excellent photophysical properties. Thus, any use in bioinspired applications requires additional chemical manipulation and processing to render them hydrophilic and biocompatible (12,21). Several strategies have been developed in the past decade to achieve this goal, yet with mixed results. These approaches can be grouped in two main strategies (umbrellas) often referred to as encapsulation and ligand exchange (Fig. 1). The first relies on encapsulation of the nanocrystals with their native hydrophobic ligands within an amphiphilic block copolymer or phospholipid micelles, whereas the second involves removing the native cap and replacing it with a set of coordinating small molecules or polymeric ligands. Although the strategy based on ligand exchange with small molecules has provided hydrophilic nanoparticles with great long-term stability that are readily functionalized with target molecules, the present article will focus on the use of polymeric molecules to promote water-solubility and biofunctionalization of the nanocrystals. This will include both types of polymers: amphiphilic polymers often used for encapsulation of the native nanocrystals, as well as those interacting through metal-affinity coordination with the nanocrystal surfaces used for ligand exchange.

The use of polymers for encapsulation or cap-exchange offers a promising approach, given the large wealth of knowledge and expertise developed over the years for preparing an array of amphiphilic polymers. Indeed such expertise has allowed several groups to synthesize and optimize numerous block copolymers with well-defined structures and control over the block size, nature, and the exact stereochemistry of the macromolecules (23,24).

We will first summarize the synthetic strategies developed over the past decade to prepare high quality inorganic nanoparticles/nanocrystals using the high temperature growth procedure where size and size dispersity are well controlled. We then highlight the recent advances in the synthesis of several amphiphilic polymers and their use to promote water solubilization by either encapsulation or ligand exchange. Finally, we will discuss some of the applications of the resulting polymer-functionalized nanomaterials in biology.

High Temperature Growth of Quantum Dots, Metal, and Metal Oxide Nanoparticles

This route relies on the reduction of organometallic precursors at high temperature and in the presence of coordinating solutions. It is applicable to a wide array of materials ranging from semiconductor QDs and magnetic nanocrystals, to gold and other metal nanoparticles. One of the key advantages of this growth route is its ability to reproducibly provide homogeneous materials with crystalline cores and low size dispersity. This has allowed researchers to carry out sophisticated experimental investigations, where fundamental photophysical, spectroscopic, and chemical properties can be probed, and the ensuing results can be tested against proposed conceptual models (21,25–31). This has also

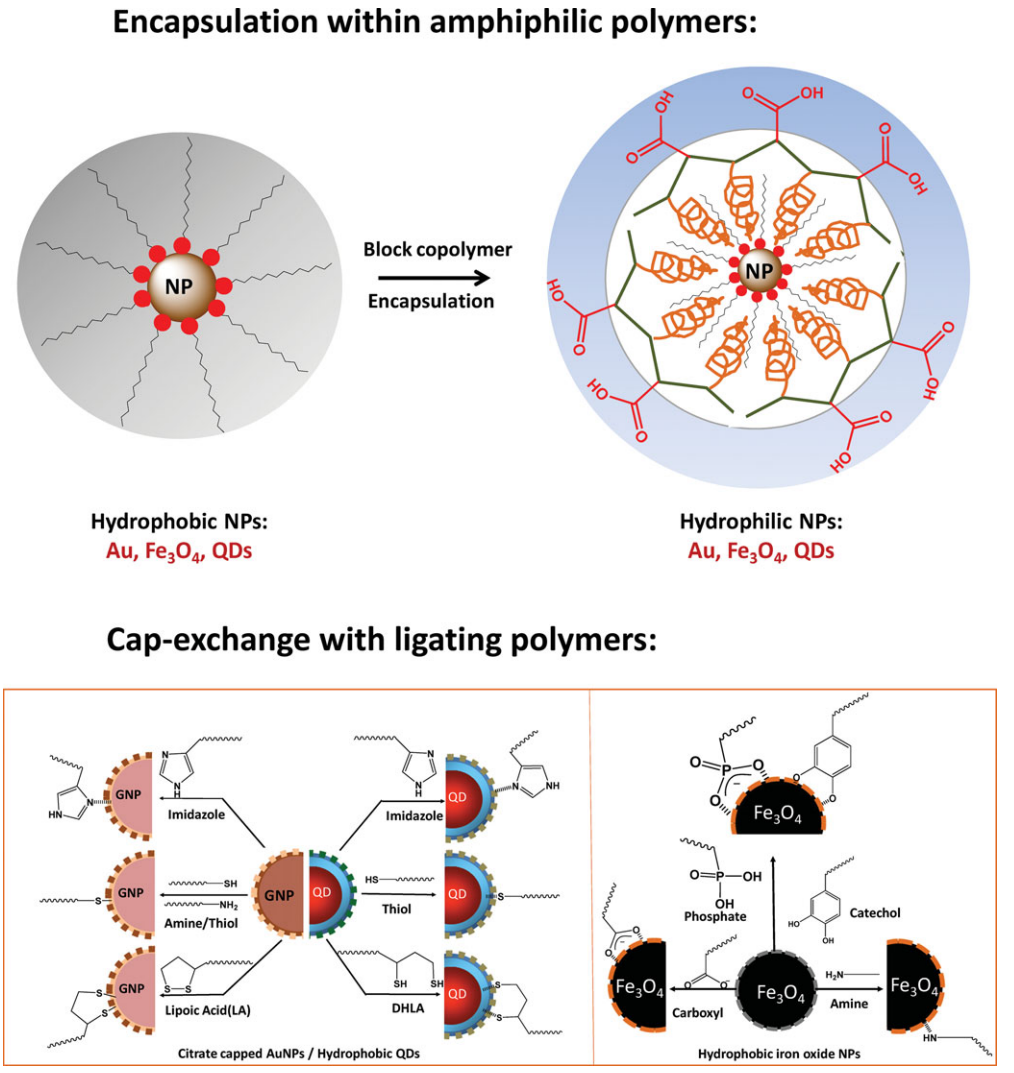

Fig. 1. (A) Schematic representation of encapsulated nanoparticles (NPs) within block copolymer; (B) Different anchoring groups for coordination onto metallic (AuNPs), semiconductor (QDs), and magnetic (iron oxide) nanocrystals.

brought these nanostructured materials closer to the realm of targeted applications, where integration into electronic, optical, and biological devices can be attempted.

Semiconductor Quantum Dots. Semiconductor QDs are nanocrystals consisting of a few hundreds to few thousands of atoms. They can be spherical, cubic, rod-like, branched, or tetrapod-like (19,32–34). One of the first studies reporting the effects of carrier confinement within the nanometer size of semiconductor nanocrystal was reported in 1981–1982, where the authors measured the optical spectra for nanometer-sized CuCl, CdS, or CdSe incorporated into

silicate glasses (35,36). A few crucial reports further confirmed the effects of carrier confinement in nanoscale structures. In 1982, Efros and co-workers showed that glass matrices containing precipitated crystallites of CdS_xSe_{1-x} can be used to build optical filters where variations in the size and/or stoichiometry of the crystallites allowed tuning of the corresponding absorption band (37). Similar results were reported by Hall and Borelli at Corning Inc (38,39). Simultaneously, the growth of colloidal QDs using reverse micelles was also reported by Brus and Heinglein and co-workers, which provided nanocrystals with size-tunable optical features that can be studied and processed from solution conditions (40–42).

However, a major development in the growth of high quality colloidal QDs was achieved by Bawendi and co-workers in 1993. They showed that high quality CdSe QDs, in terms of core crystallinity, low size dispersity, and brightness, can be prepared by high temperature reduction (or hot injection) of dimethyl cadmium ($CdMe_2$) and trioctylphosphine-selenide (TOP:Se) in a hot coordinating solution (at 280–350°C) of trioctylphosphine and trioctylphosphine oxide (TOP/TOPO) (19). In particular, they showed that the nanocrystals exhibit narrow and size-tunable symmetric photoluminescence (PL) spectra, high molar extinction coefficient and high photo- and chemical stability. In subsequent studies, Peng and co-workers refined the synthesis by introducing new cadmium precursors (eg, CdO and $Cd(AC)_2$) that are less volatile and easily storable under ambient conditions (43,44). They also showed the importance of introducing additional strong coordinating molecules such as alkyl-amine and alkyl-carboxy to the growth reaction. A flurry of reaction modifications and adjustments followed those studies where several groups have further optimized the growth conditions and expanded those ideas to the growth of other nanocrystals (22,45–47). These combined studies have also shown that the photophysical properties of the QDs can be improved by overcoating the native core with a shell made of a few monolayers of wider band gap semiconducting material such as ZnS or ZnSeS (48,49). Among all the QDs reported so far, CdSe QDs overcoated with ZnS or ZnSeS provide the best photophysical properties and thus are the most popular QDs for biomedical sensing and imaging.

Iron Oxide Nanoparticles. The growth of magnetic nanoparticles (such as those made of iron oxide cores) initially relied on the precipitation of Fe-salts, namely $FeCl_3$ in hydrophilic media, and materials prepared through this route have been used in a variety of studies (50–52). Although this route provided effective means to prepare the hydrophilic nanoparticles, control over the nanoparticle size, core crystallinity and size dispersity was marginally achieved.

Following the advent of high temperature reduction method for QDs, several groups expanded this route to grow magnetic nanocrystals (7,21,53–60). In one of the earlier growth methods reported by Hyeon and co-workers, the authors started by developing an organometallic iron complex, iron-oleate, prepared by reacting iron chloride ($FeCl_3{\cdot}6H_2O$) and sodium oleate in a mixture of ethanol, water, and hexane at ~70°C for 4 h (21). Following several washes with distilled water and evaporation of the organic solvent(s), a waxy solid compound is obtained, which can be stored for further use. In a typical reaction to grow 12-nm nanoparticles, the iron-oleate is dissolved in a noncoordinating organic solvent (eg, 1-octadecene) and the mixture is heated to ~320°C. After 30 min at this temperature, the transparent colorless solution becomes turbid and brownish black,

indicating the formation of iron oxide nanoparticles. The size of the nanoparticles can be controlled by using various solvents with different boiling temperatures, with larger size nanocrystals obtained for solvents with higher boiling points. This route has provided hydrophobic dispersions of homogeneous iron oxide nanocrystals with tunable size, low size distribution, and crystalline cores. It has further been expanded to prepare metal-doped iron oxide nanoparticles with enhanced coercivity, and the resulting nanoparticles were applied for visualizing (through magnetic resonance imaging, MRI) a few specific biological events (57,61).

Gold Nanoparticles. The growth of Au nanoparticles (AuNPs) using chemical reduction of gold precursors at room temperature in either an aqueous or biphasic water-organic solution has been effectively used by several groups and has evolved over the years (2). In one of the early pioneering studies, Turkevitch and co-workers first reported the growth of ~12 nm AuNPs using reduction of chloroauric acid in water using trisodium citrate (62). Frens further enabled the control over the AuNPs size from 16 to 140 nm by varying the citrate-to-gold precursor ratio (63). A major development in this field was the synthesis of hydrophobic AuNPs functionalized with alkane thiol using the two-phase (toluene/water) approach reported by Brust and Schiffrin (64). In their method, $HAuCl_4$ was transferred from the aqueous phase to toluene (organic phase) using the surfactant tetraoctylammonium bromide and reduced by sodium borohydride ($NaBH_4$) in the presence of dodecanthiol. Recently, our group has developed one phase growth of AuNPs capped with a series of dithiol-terminated molecules, lipoic acid (LA)-based modular polyethylene glycol (LA-PEG) or sulfabetaine zwitterion (LA-ZW) ligands, with a control over the size of the nanoparticles ranging from 2 to 20 nm (65,66). There have also been instances where various polymers such as poly(*N*-vinylpyrrolidone), poly(4-vinylpyridine), poly(vinyl alcohol), polyethyleneimine (PEI), and poly(diallyl dimethylammonium chloride) have been used to grow and to stabilize the nanoparticles (67–69). However, recent studies have shown that the hot injection method provides better quality and more homogeneous AuNPs, as it has been demonstrated for many types of semiconductor nanocrystals.

Another approach for synthesizing and controlling the size and shape of AuNPs is the seed-mediated growth. Here, small metal nanoparticles are prepared first and then used as seeds (nucleation centers) for growing larger size AuNPs as well as Au nanorods (AuNRs) (70,71). This is an effective and easy approach for preparing AuNRs with varying aspect ratio, which finally reflects the position of the plasmonic peak in the absorption spectra (72). So far, thiol-containing compounds have been widely used as protective agents for obtaining stable monolayer-protected AuNPs, because of the strong affinity of sulfur to gold (73).

Surface-Functionalization Strategies

Postgrowth surface-functionalization of the nanocrystals/nanoparticles is paramount to integrate these systems with biology. This requirement is valid regardless of the initial growth method used or the nature of the inorganic

nanocrystals. For instance, citrate-capped AuNPs and cetyl trimethylammonium bromide (CTAB) coated AuNPs and AuNRs, though water soluble as prepared, exhibit limited colloidal stability to added electrolytes and pH changes, which limits one's ability to easily integrate them with proteins and peptides or introduce them into live cells. Thus, additional surface-modification steps have been used to expand their colloidal stability and impart biological activities to these materials. For materials prepared using high temperature growth in hydrophobic solutions, a judicious surface-functionalization strategy is critically important and can promote water-solubility and biofunctionality to the nanocrystals.

Overall, the strategies developed for achieving surface-functionalization and biocompatibility can be grouped into two main approaches (see Table 1): (1) encapsulation of the native hydrophobic nanocrystals with amphiphilic molecules (74–77) and (2) exchanging the native hydrophobic ligands with bifunctional molecules (78–83). The first relies on the entropy-driven interdigitation between the hydrophobic segments of the amphiphilic molecules and the native cap on the nanocrystals, while leaving the hydrophilic lateral blocks (segments) free to interact with the surrounding buffer. Conversely, because ligand (or cap) exchange entails the removal of the native cap, it requires the bifunctional molecules to present one or multiple coordinating groups to anchor onto the inorganic surface; the hydrophilic functions promote affinity to water. In either strategy, polymers have provided researchers with a great variety of structures to work with. For example, several block copolymers exhibit critical micelle concentration very close to zero, which makes them stable under a wide range of physiological conditions and suitable for therapeutic applications (84). In addition, there has been a wealth of available chemical routes for judiciously introducing new functional and/or coordinating groups in the polymer macromolecules for optimal functionalization of the nanocrystals (23,24).

Encapsulation within Amphiphilic Block Copolymers. Since this strategy requires the presence of two distinct blocks with drastically different solubility properties, a balance between the hydrophilic and hydrophobic blocks is crucial for its effectiveness. In the following, we will describe a few representative examples where this strategy was applied to the encapsulation of AuNPs and nanorods, followed by semiconductor QDs and magnetic nanocrystals.

Encapsulation of Gold Nanoparticles. Compared to their magnetic and semiconducting nanocrystal counterparts, encapsulation of metal nanoparticles (Au and Ag) has been less commonly used. In one study, Kang and Taton used atom-transfer radical polymerization to synthesize and optimize two amphiphilic block copolymers that share a common poly(acrylic acid) (PAA) hydrophilic block, but two different hydrophobic blocks: a polystyrene-*block*-poly(acrylic acid), PS-*b*-PAA, and poly(methyl methacrylate)-*block*-poly(acrylic acid), PMMA-*b*-PAA. They showed that these two polymers can be used to encapsulate dodecanethiol-modified (hydrophobic) AuNPs (85). Here, the nanoparticles were first cap-exchanged with dodecanethiol to promote interdigitation with the hydrophobic segments of the block copolymers and formation of the micelle capsules around the nanoparticles, once water was added to a DMF solution containing the polymer mixed with the nanoparticles. They then used 2,2′-(ethylenedioxy)bis(ethylamine) to cross-link the PAA block to provide stable surface coating to the nanoparticles. In another study, these authors expanded

Table 1. Summary of the Various Surface-Functionalization Strategies Developed Thus Far for Either Nanoparticle Encapsulation or Ligand Exchange Using a Variety of Polymer Structures and Configurations

Strategy	Polymer Used	Type of the Nanoparticle Used	Reference
Encapsulation	Poly(styrene-*block*-acrylic acid) or poly(methyl methacrylate-*block*-acrylic acid)	Au	(85)
	[Polystyrene-*co*-poly(4-vinyl benzophenone)]-*block*-poly(acrylic acid)	Au	(86)
	Poly(ethylene oxide)-poly(*n*-butyl acrylate)	Au	(88)
	PAA modified with alkylamine	CdSe–ZnS, Au	(76,87)
	Poly(maleic anhydride-*alt*-1-tetradecene)	Au, CdTe, CdSe–ZnS, Fe_3O_4, $CoPt_3$	(77)
	Poly(maleic anhydride-*alt*-1-octadecene) modified with amino poly(ethylene glycol)	CdSe–ZnS, Fe_3O_4	(75)
	Poly(styrene-*co*-maleic anhydride) modified with amino PEG (Jeffamine)	CdSe–ZnS, Au, Fe_3O_4	(102,104)
Cap-Exchange	Methacryloyloxyethyl phosphorylcholine block copolymer	Au	(130)
	Poly(L-lysine)-*graft*-poly(ethylene glycol)	Au	(124)
	Poly(acrylic acid)-*graft*-mercaptoethylamine	CdSe–ZnS	(125)
	Poly(acrylic acid)-*graft*- OligoPEG-LA/DHLA	Au, CdSe–ZnS	(128)
	LA/DHLA-*graft*-polymethacrylate	CdSe–ZnS	(126,127)
	DHLA/zwitterion-*graft*-polymethacrylate	CdSe–ZnS	(129)
	Poly-poly(ethylene glycol)-poly(imidazole)	CdSe–CdS	(81,132,133)
	Polydimethylaminoethyl methacrylate (PDMA)	CdSe–ZnS	(105)
	Poly(acrylic acid)-*graft*-OligoPEG-DOPA	Fe_3O_4	(140)
	Polyethylenimine-*graft*-polyDOPA	Fe_3O_4	(141)

their strategy and synthesized two photo-cross-linkable polymers, [polystyrene-*co*-poly(4-vinyl benzophenone)]-*block*-poly(acrylic acid) [(PS-*co*-PVBP)-*b*-PAA] and [poly(styrene)-*co*-poly(4-vinyl benzophenone)]-*block*-poly- (ethylene oxide) [(PS-*co*-PVBP)-*b*-PEO] (86). They showed that with both polymer designs, the resulting encapsulated nanoparticles exhibit great thermal and colloidal stability to pH changes and added salts, and can be further functionalized with biomolecules. In another example, Kairdolf and Nie used an amphiphilic polymer made of a PAA chain in which 40% of the carboxyl groups were modified with a 12-carbon aliphatic chain (dodecylamine) for the *in situ* growth of AuNPs. In their polymer-coated nanoparticles, they suggested that this amphiphilic polymer forms a three-layer coating on the nanoparticles, with a hydrophobic layer resulting from the self-assembly of two polymer chains, intercalating between two carboxyl-rich lateral layers: One of the carboxy-rich layers coordinates onto the metal surface, whereas the other one interacts with the surrounding water, promoting dispersion of the nanoparticles in alkaline solutions. They found that the polymer capsules exhibit pH-dependent structures, where shedding of the polymer outer layer in acidic pH alters the nanoparticles solubility (nanoparticles become compatible with nonpolar media) along with a decrease in the hydrodynamic radius (87). The encapsulation strategy has also been applied to AuNRs, though with less frequency. For example, Kim and co-workers utilized a poly(ethylene oxide)-poly(*n*-butyl acrylate), PEO-P*n*BA diblock copolymer to encapsulate CTAB-capped AuNRs (88). The hydrophobic P*n*BA chains were found to have a strong affinity to the gold surface, which helped the formation of dense micelle assemblies onto the Au surface, whereas the poly(ethylene oxide) chains provided high water solubility to the nanorods. Finally, adsorption of polyelectrolytes, either as or by layer-by-layer self-assembly has been used to functionalize citrate-coated AuNPs and nanorods (89,90). This may be qualified as another form of encapsulation within polymeric materials.

Encapsulation of Magnetic Nanoparticles and Quantum Dots. Implementation of this strategy to QDs and magnetic nanocrystals has been more widely used than for other types of nanocrystals. Indeed over the past decade, several studies have explored a variety of either commercially available or custom-modified block copolymers to encapsulate an array of hydrophobic semiconductor and iron oxide nanocrystals alike (91–94). To prepare such amphiphilic polymers, researchers mainly targeted three types of backbones for further modifications: PAA, polydimethylaminoethyl methacrylate (PDMA), and polymaleic anhydride, even though other systems were also used. These polymers present along their backbones easy to modify reactive groups, such as carboxyl and maleic anhydride (through simple transformations), for further insertion of hydrophilic and/or hydrophobic block into the overall structures. This can allow one to tune the balance between the hydrophobic and hydrophilic blocks, thus controlling the overall behavior of the amphiphilic polymer. In one of the early demonstrations, Wu and coworkers detailed the use of a PAA chain where 40% of the carboxyl groups were modified with octylamine to encapsulate CdSe-ZnS QDs (76). For this system, the hydrophobic octyl side chain interdigitated within the native TOP/TOPO ligands (through hydrophobic attractions) whereas the remaining negatively charged carboxy groups promoted water compatibility. The resulting QDs were further cross-linked through a 1-ethyl-3-(3-dimethylaminopropyl)carbodiimide (EDC)

condensation reaction, with lysine or polyethylene glycol (PEG) lysine, followed by a reaction with antibodies or streptavidin to render these nanocrystals bioactive. These nanocrystals were in fact the first commercially offered biocompatible QDs, and they were used in an array of reported studies over the past decade (76,95–101). Using a similar approach, Nie and co-workers used a commercially available high molecular triblock copolymer consisting of polybutylacrylate, polyethylacrylate, and a polymethacrylic acid segments, on which they grafted a few eight-carbon (C-8) alkyl side chains (as the hydrophobic modules). They then showed that the inserted alkyl segments allow the encapsulation of TOP/TOPO-QDs within this triblock copolymer, whereas the carboxyl groups permitted further coupling to antibodies and tissue labeling (92). Parak and co-workers introduced the use of poly(maleic anhydride-*alt*-1-tetradecene) (M_w = 30,000–50,000) as a flexible platform to prepare amphiphilic polymers to encapsulate various inorganic nanocrystals (Fig. 2) (77). The polymer was initially adsorbed onto the hydrophobic QDs in an organic solution (eg, chloroform), followed by addition of bis(6-aminohexyl) amine to form cross-linked polymer capsules around the nanocrystals. Mixing the dried QDs with water-promoted hydrolysis of the unreacted anhydride units, which allowed readily dispersion of the QDs in aqueous media, driven by the newly available carboxylic acids along the polymer backbone. They also showed that this approach can indeed be applied for the encapsulation of QDs, iron oxide, gold, and CoPt nanoparticles (Fig. 2**A**) (77). In a subsequent study, they coupled ATTO-dye molecules premodified with the amino group to the alkyl-modified polymer backbone; they then used these hybrid complexes to probe the energy transfer interactions between QDs and dyes, and their dependence on the environment conditions (74). A few more recent studies have expanded on this idea and inserted PEG segments into the polymer structure to improve the QD biocompatibility and eventually reduce nonspecific interactions. In particular, Colvin and co-workers introduced lateral PEG chains onto the polymer prior to mixing with the nanocrystals (75). They first reacted poly(maleic anhydride-*alt*-1-octadecene) with amine-modified methoxy-terminated poly(ethylene glycol) (NH_2-PEG-OCH_3) to form the amphiphilic polymer. The nanocrystals and polymer were then mixed in chloroform, followed by addition of buffer after drying the organic solvent, which produced hydrophilic QDs or iron oxide nanoparticles. In another study, Mulvaney and co-workers used an amphiphilic polymer, poly(styrene-*co*-maleic anhydride) (M_w = 1700), which was made by maleic anhydride coupling to either ethanolamine or the amino-PEG derivative Jeffamine M-1000 polyetheramine. The resulting water-soluble nanocrystals presented both PEG moieties and COOH groups on their surfaces (102). In a subsequent study, the authors introduced azide groups into the polymer structure and tested the ability to conjugate the resulting azide-functionalized QDs to cyclooctyne-modified transferrin (a protein) or cyclooctyne-modified Alexa Fluor 594 (a fluorescent dye), using copper-free strain-promoted azide-alkyne cycloaddition (SPAAC), previously developed by Jewett and Bertozzi (103). The cycoloctyne was attached to the dye or the protein through a bifunctional linker bearing an electrophilic ethyl squaramate group; the latter reacts with lysines or amines on the target (eg, protein). They demonstrated that the number of azide groups on the polymer-encapsulated QDs can be simply controlled by varying the molar ratio between the amine-PEG-azide and

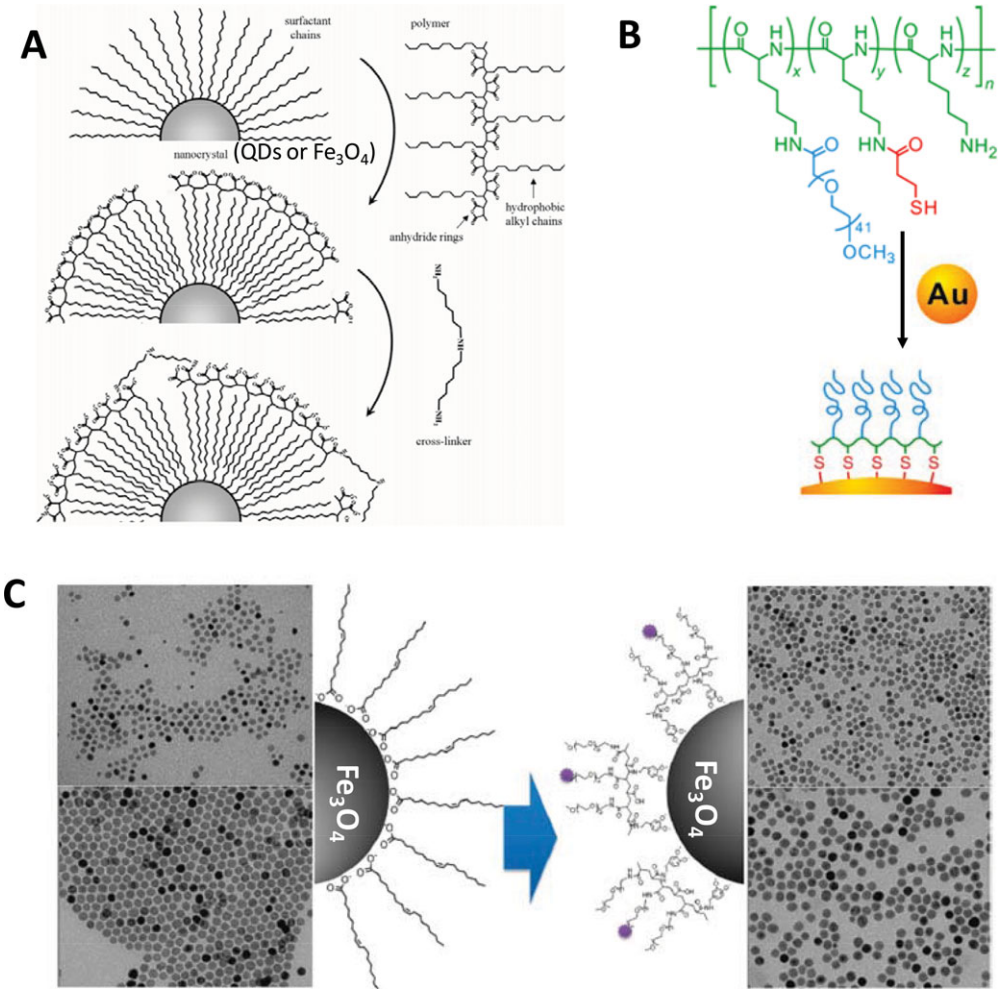

Fig. 2. A few representative schemes used for the phase transfer and applied to (**A**) encapsulation of QDs and iron oxide nanocrystals within amphiphilic polymers (77), (**B**) ligand exchange of AuNPs using thiol-to-Au coordination (124), or (**C**) ligand exchange of iron oxide nanoparticles using OligoPEG-dopamine ligands (140). Reproduced from Refs. (77), (124), and (140), with permission from the American Chemical Society.

amine-PEG-methoxy moieties introduced along the polymer backbone (104). They further tested the biological activities of SPACC-promoted QD-transferrin conjugates by monitoring their uptake by cells expressing transferrin receptors on their membranes. These studies clearly show that the maleic anhydride motif provides a great platform to prepare several tailor-made block copolymers by introducing hydrophobic as well as hydrophilic moieties (short alkyls and PEG moieties) and inserting the desired functionalities. In related approaches, PEG-grafted polyethylenimine (PEI-*g*-PEG) and diblock copolymer poly(ethylene glycol-*b*-2-*N*,*N*-dimethylaminoethyl methacrylate) (PEG-*b*-PDMA) were used to promote the transfer of QDs to buffer media (105–107). Nonetheless, in these

reports the authors have attributed the affinity between the polymer and the inorganic surface of nanocrystals to the removal of native ligands by ionic anchors in the polymer. Cyclic molecules such as calix[*n*]arene (with $n = 4, 6, 8$) containing carboxylic acid groups were also used to encapsulate luminescent QDs (108). Weller and co-workers described a few interesting developments based on block copolymer design to encapsulate individual or combinations of inorganic nanocrystals and promote their transfer to buffer media (109,110). In an earlier study, they detailed the use of a chemically designed triblock copolymer to cap CdSe–ZnS QDs through partial ligand exchange. The polymer consists of a polyethyleneimine-binding block (to promote an interaction with the inorganic surface through amine binding), a hydrophobic polycaprolactone, and a PEG block that facilitates dispersion of the nanoparticles in aqueous media (111). The authors explored the effects of varying the size of the three blocks and showed that ^{1}H NMR could provide an effective tool for tracking polymer binding onto the QDs and progressive removal of the native TOPO cap. They also found that varying the polymer-to-nanoparticle molar ratio could lead to the formation of polymer capsules containing either individual nanocrystals or beads of multiple nanocrystals. In a more recent study, starting with the native hydrophobic nanocrystals they employed *in situ* seeded emulsion polymerization to prepare ethylene oxide glycol coated nanocrystals (such as nanocrystals encapsulated within an amphiphilic polyisoprene-*block*-poly(ethylene oxide) diblock copolymer (PI-*b*-PEO)) that also present multiple surface functionalities. With this *in situ* strategy, a number of combinations of the surfactants, functional monomers, linkers, and radical initiator are sequentially introduced along with the nanocrystals to promote the encapsulation of one type or a combination of nanocrystals within the same capsule (112).

Ligand Exchange. Since this strategy involves the removal of the native coating (eg, CTAB, oleic acid, and TOP/TOPO) and its replacement with bifunctional hydrophilic ligands, a judicious choice of the polymer ligand must combine high affinity anchoring groups, hydrophilic blocks, and reactive groups. These parameters control the stability of the inorganic nanocrystal-to-ligand binding and colloidal stability of the resulting dispersions, whereas the reactive groups allow one to apply the optimal coupling strategy to attach the desired number and type of target molecules (eg, peptides and proteins). The choice of the anchoring groups depends on the nature of the inorganic nanocrystals (Fig. 1) (113–118). For example, while dopamine has been shown to provide strong coordination onto the surface of iron oxide nanoparticles, its ability to coordinate onto Au and semiconductor surfaces is rather weak. Conversely, thiols moieties exhibit much stronger affinity to AuNPs and Zn-rich QD surfaces. Indeed, Au-to-thiol (or Au-sulfur) interaction has been referred to in several instances as a covalent attachment (119) and thiol-appended ligands are believed to be the most effective for functionalizing AuNPs and AuNRs (120–122). Carboxy and amine groups have also been proposed as anchoring groups onto Au, iron oxide, and QD surfaces, although their effectiveness seems to be much better confirmed when nanocrystals are grown using high temperature reduction routes and are capped with alkylamine and alkylcarboxy ligands in organic solutions. More recently, a few studies have shown that a polyhistidine (namely, the imidazole group in the

aminoacid histidine) inserted into polymer structures exhibits strong affinity to AuNPs and core–shell QDs (81,117).

Gold Nanoparticles and Semiconductor Quantum Dots. Ligand exchange on AuNPs and QDs using thiol-appended alkyl and thiol-modified PEG molecules has been used by several groups over the past decade. Indeed, most of the earlier studies focused on QDs ligated with mono- and dithiol-appended ligands (eg, mercaptoacetic acid, 11-mercaptoundecanoic acid, and dihydrolipoic acid, DHLA) (78,83,123). All these small molecules are commercially available, and the cap exchange procedure is easy to implement. However, the QDs cap exchanged with those small molecules (carboxy terminated) suffer from limited long-term colloidal stability in buffer media especially in acidic conditions. In addition, colloidal stability of the resulting QD dispersions largely depends on the exact structure of the ligand used and the strength of its coordination onto the nanocrystal surface. For instance, derivatives of DHLA-appended PEG provide substantially better stability and reactivity than their monothiol-alkyl counterparts, a feature attributed to the stronger binding affinity of the dithiol group to the Zn-rich surface of the CdSe-ZnS QDs (80,83). Learning from the effectiveness of higher coordination onto metal surfaces, polymer structures present an obvious platform for preparing ligands with greatly enhanced ligand-to-nanocrystal coordination (ie, multidentate ligands). In the following, we will detail a few representative examples relying on the use of thiol-modified polymers for ligand exchange onto AuNPs and QDs.

When employing this strategy for AuNPs, the most commonly used starting materials are citrate- or CTAB-stabilized nanoparticles. The use of multicoordinating functional block copolymers to cap AuNPs has recently been explored by a few research groups, where several monothiol- or dithiol-terminated ligands are grafted onto an alkyl backbone. For example, one of the recent reports by Kang and Taton described the synthesis of poly(L-lysine)-*graft*-poly(ethylene glycol) (PLL-*g*-PEG) copolymers having both mono-thiol-terminated ligand and methoxy-terminated PEG chain and tested their effectiveness to passivate and disperse AuNPs in buffer media (124). In their methods, several thiol groups and PEG chains were incorporated into the poly(lysine) backbone by sequential addition of *N*-hydroxy succinimide (NHS)-ester-terminated PEG-(mPEG-SCM) and thiol-linker (*N*-succinimidyl-3-(2-pyridyldithio)-propionate); the chemical reaction relied on amide bond formation through ester-amine coupling (Fig. 2**B**). In addition, by leaving a few of the amine groups in the lysine residues intact, this could permit further coupling of the nanoparticles to biomolecules (124). Liu and co-workers targeted carboxyl groups on PAA for a reaction with mercaptoethylamine to prepare multithiol-modified polymer ligand, which was used to transfer QDs to buffer media (125).

Instead of monothiols, a few groups grafted lipoic acid (dithiolane) or lipoic acid modified with a short PEG segment onto the polymer backbones. For example, Raymo and co-workers designed a polymer construct made of polymethacrylate backbone, presenting several lateral LA groups to solubilize the hydrophobic QDs (126,127). Their synthetic strategy was based on the radical copolymerization of methacrylate monomers prefunctionalized with lipoic acid and PEG moieties with varying chain lengths, or PEG moieties presenting lateral amine or carboxyl groups (Fig. 3**B**). The authors showed that following

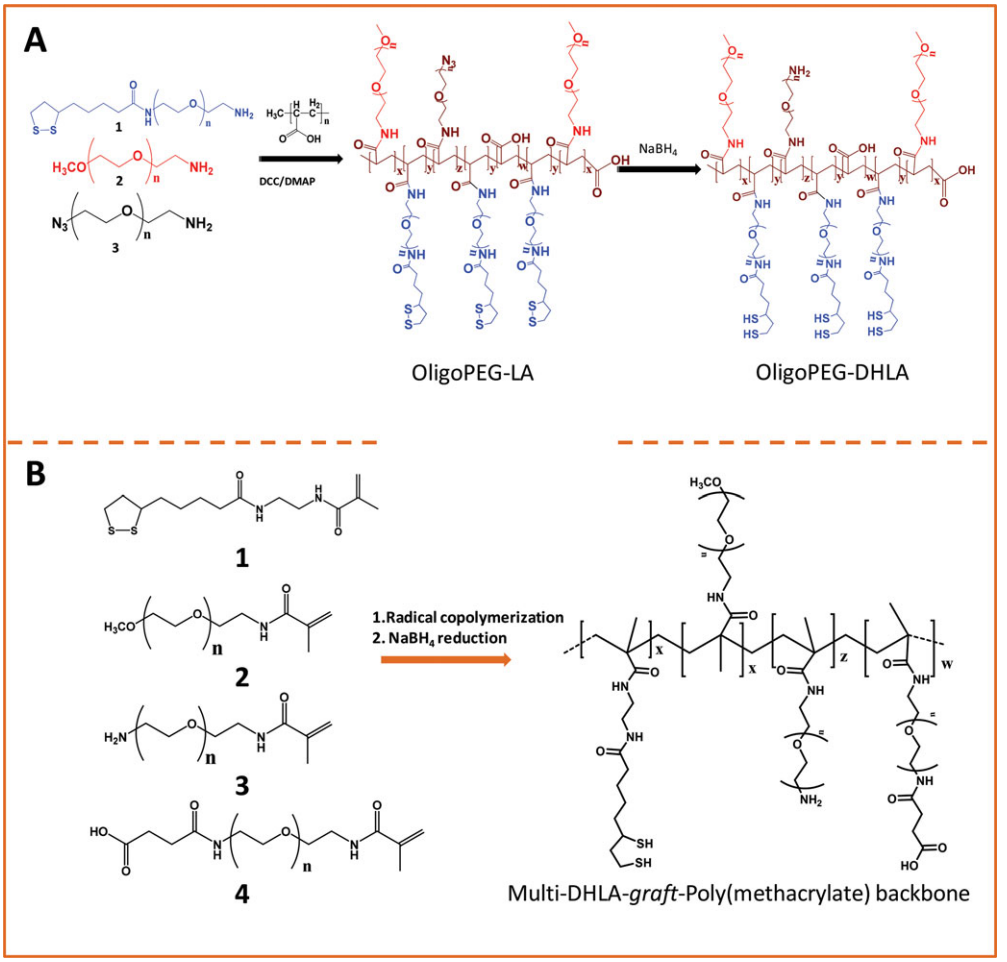

Fig. 3. Synthetic scheme used for preparing block copolymers presenting multiple lipoic acid (or DHLA) anchoring groups laterally grafted onto an aliphatic chain using (**A**) a PAA (128) or (**B**) a polymethacrylate (126) as a backbone. Schemes reproduced from Refs. 128 and 126, with permission from the American Chemical Society.

borohydride reduction of the LA groups, the resulting polymer ligands provided QDs with enhanced long-term stability compared to monothiol small ligands. They further showed that the availability of the functional groups allowed subsequent functionalization with target molecules (bio and others). Here the larger PEG chain tended to increase the effective hydrodynamic size of the water-dispersible QDs. To produce nanocrystals with smaller hydrodynamic size, a few groups used PAA oligomers (with molecular weight of ~1800) (128). For example, our group used this PAA short chain as platform to prepare a series of PEG- and LA-modified oligomer ligands having a central backbone laterally appended with combinations of LA-PEG, methoxy-PEG, amine-PEG, and azide-PEG moieties (OligoPEG ligands) (128). We used shorter PEG moieties (M_w ~600 or 750) to eventually reduce the overall extension of the polymer coating on the

nanocrystals (Fig. 3**A**). These LA-modified OligoPEG ligands were applied either to cap AuNPs or to functionalize QDs after borohydride reduction (128). This route provided colloidal dispersions of QDs and AuNPs that remained stable over a broad range of conditions and extended periods of storage time. Giovanelli and co-workers took a slightly different approach for achieving multicoordination while maintaining compactness of the ligands (Fig. 4). They synthesized a hydrophilic polymer containing molecular lipoic acid anchors and a sulfobetaine zwitterion groups by a two-step process. They first modified the lipoic acid and zwitterion with methacrylamides and then performed the polymerization reaction to obtain a randomly grafted copolymer (129). The authors showed that this multi-LA-appended polymer exhibits strong affinity to QD surfaces, with reduced desorption rates compared to their lower coordination ligand counterparts. Recently, Emrick and co-workers combined the zwitterion (instead of PEG) moieties along with multiple lipoic acid to synthesize methacryloyloxyethyl phosphorylcholine block copolymer by free radical polymerization (Fig. 4) (130). They showed that this polymer ligand was effective for displacing CTAB from AuNR surfaces and providing water dispersions with great colloidal stability.

Although the ligand exchange using imidazole moieties as anchoring groups has not been actively pursued, a few recent studies reported the ability of imidazole-modified ligands, or polyhistidine-appended peptides and proteins to effectively interact with core–shell QDs and AuNPs (81,131). Conjugation of hydrophilic QDs to polyhistidine (His_n)-tagged proteins and peptides, promoted by metal-affinity interactions, has been explored by several groups, due to the ease of implementation and the fact that His-tagged biomolecules are ubiquitous. We have, for instance, demonstrated the conjugation of CdSe-ZnS QDs with His-tagged proteins and peptides and showed that such interactions require direct access of the polyhistidine tag to the Zn-rich QD surfaces (131). Bawendi and co-workers exploited this idea and designed a random brush copolymer having both PEG and imidazole as side groups along its aliphatic backbone, through a radical addition-fragmentation chain transfer (RAFT) polymerization reaction (81). To minimize the potential for polymer cross-linking and aggregation of QDs after ligand exchange, the molecular weight of the final polymer was kept small by targeting degrees of polymerization below 30. They also varied the molar ratios of the various monomer precursors along with the RAFT reagent to control the final number of imidazole anchors and PEG moieties in the final polymer ligand (Fig. 4). They showed that this imidazole-rich polymer can effectively displace the native TOP/TOPO cap and coordinate onto QD surfaces, providing water-dispersible relatively compact QDs with long-term stability at pH > 5 (81). They further extended that design and replaced the PEG moieties with zwitterion groups (132). Another example of using the imidazole-modified polymer as a ligand for QDs was reported by Zhang and co-workers. They reacted polymaleic anhydride with histamine and N_3-PEG-NH_2 to provide azide-functionalize QDs (133). They were able to conjugate these azide-functionalized QDs to the Baculovirus through a metal-free "Click" reaction and test their uptake into A549 cells.

Magnetic Nanoparticles. A range of different anchoring groups (such as phosphonic acid, carboxy, dopamine) can be used to stabilize iron oxide nanoparticles in organic media (134–138). In fact, one of the most successful reactions

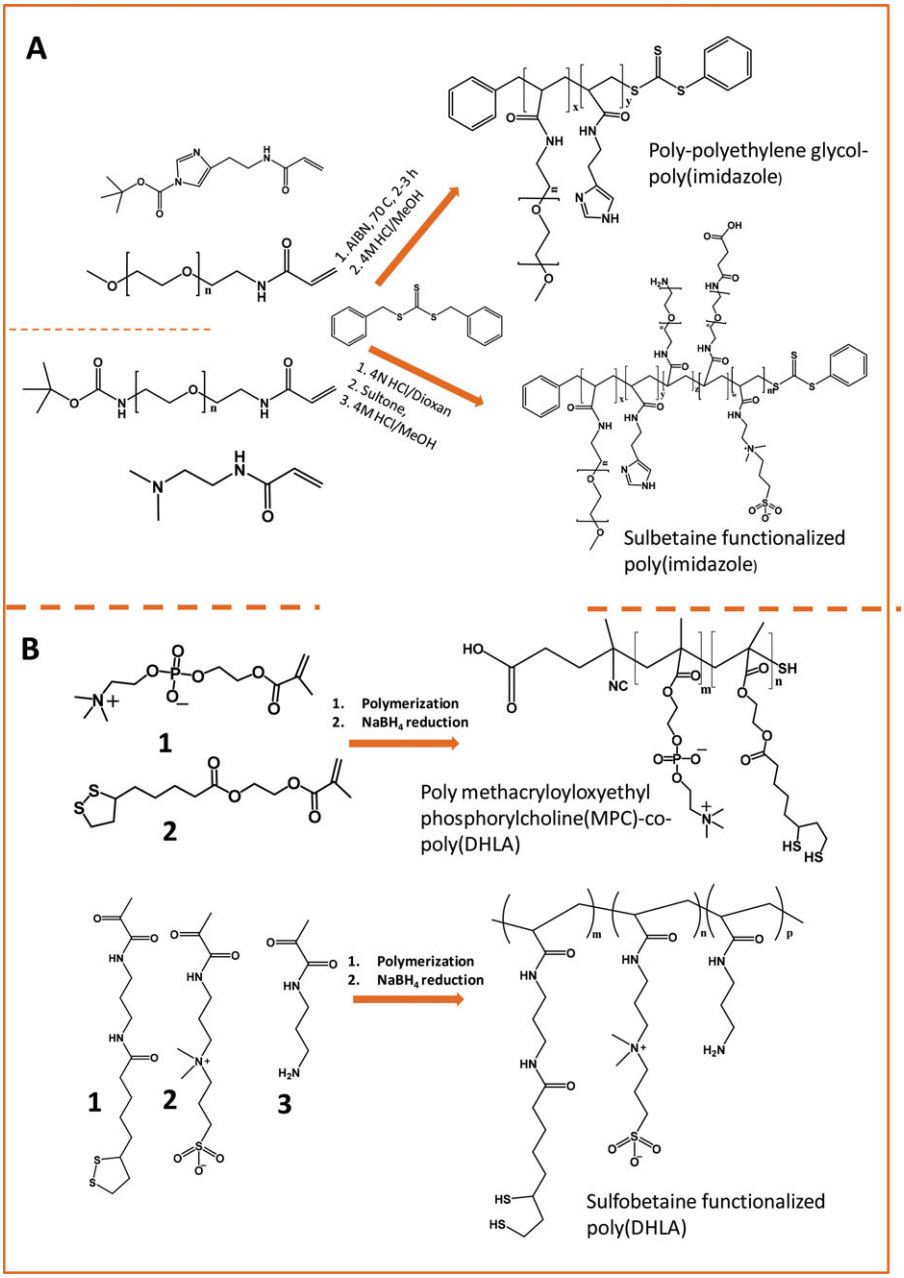

Fig. 4. Synthesis scheme use for preparing (**A**) poly(imidazole) and sulfobetaine-functionalized copolymer by RAFT polymerization using precursors (or fragments) presenting both PEG moieties and imidazoles followed by sulfobetaine coupling (reproduced from Refs. (81) and (132); (**B**) poly(LA)-zwitterion ligand relying on the polymerization of premodified zwitterion and lipoic acid precursors (reproduced from Refs. (129) and (130). Figures reproduced with permission from the American Chemical Society.

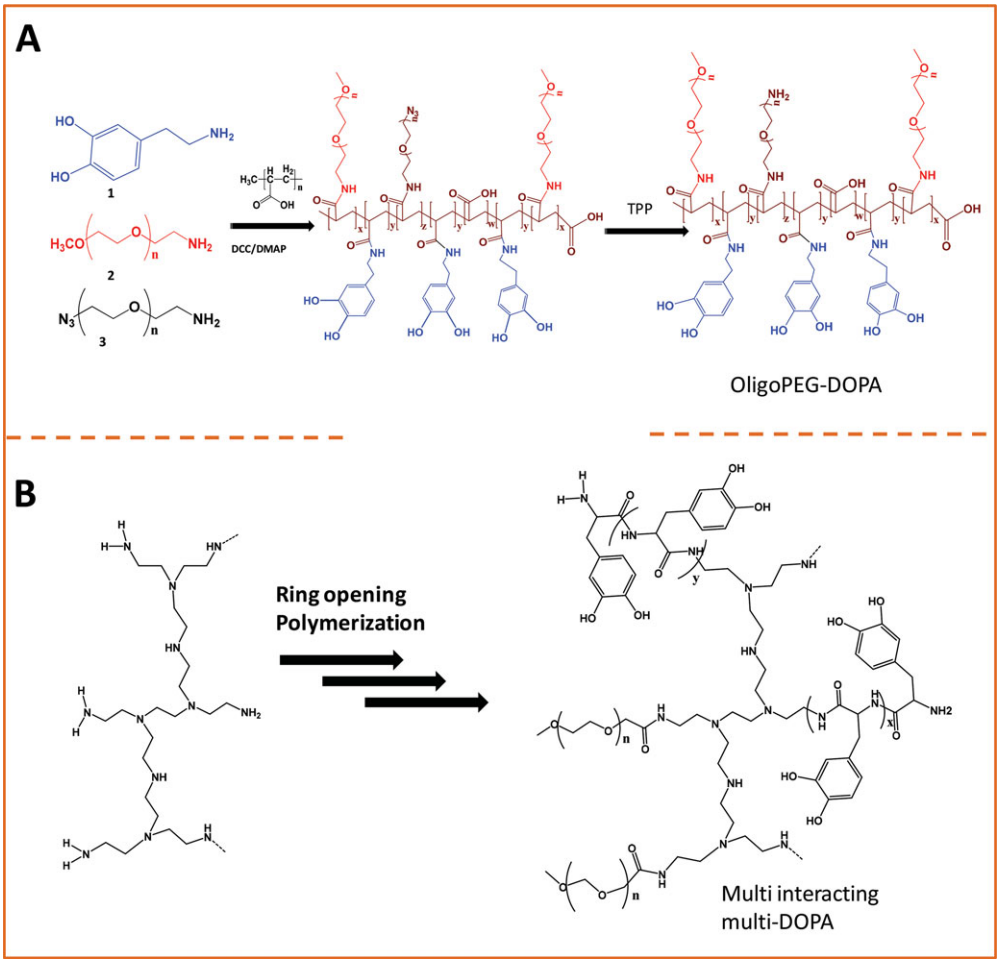

Fig. 5. Multicatechol-grafted copolymer using either (**A**) PAA as a backbone (reproduced from Ref. (140) or (**B**) hyperbranched polyethylenimine (bPEI) as the backbone (reproduced from Ref. (141). Figures reproduced with permissions from the American Chemical Society and Wiley-VCH Verlag GmbH & Co. KGaA.

to prepare high quality iron oxide nanoparticles relies on the use of oleic acid as coordinating ligand precursors (21). Several studies reported the use of catechol-appended single chain PEG to promote the transfer of iron oxide nanoparticles to water media (139). However, the stability of the resulting nanoparticles is rather limited, which has motivated a few groups to explore the design of catechol-based polymers to enhance the ligand affinity to the iron oxide nanocrystals. We have compared the effectiveness of several catechol-modified or carboxy-modified oligomers as ligands to functionalize Fe_3O_4 nanoparticles (140) (Fig. 5). In this study, poly(ethylene) glycol short chains terminated by inert (OCH_3) or functional groups were coupled laterally onto a PAA oligomer; single chain PEG modified with either one catechol or one carboxy group provided

control systems. Our results showed that the OligoPEG-DOPA ligand imparts better colloidal stability to iron oxide nanoparticles than OligoPEG-carboxy or small molecule ligands appended with carboxy or dopamine in acidic and basic buffers and to added salts. We also showed that insertion of azide groups in the oligomer allow CLICK coupling with alkyne-modified dye molecules. In another report, Hyeon and co-workers developed a multicatechol polymer ligand made of poly(L-3,4-dihydroxyphenylalanine), polyDOPA, further modified with methoxy PEG units (Fig. 5**B**). Here too, the authors reported enhanced stability of the iron oxide nanoparticles in buffer media. They also applied these nanoparticles intravenously to live mice and tracked (through MRI) the biodistribution of the functionalized iron oxide nanoparticles in specific organs such as spleen and liver (141).

Biomotivated Applications

Bioconjugation. Assembling biomolecules (eg, proteins and peptides) onto the nanoparticle surfaces is essential for using these materials in various biological applications. Several chemical strategies have been applied to conjugate the hydrophilic nanoparticles to an array of target proteins and peptides: (1) EDC/NHS (*N*-hydroxy succinimide) or sulfo-NHS coupling between carboxy functionalized dots and amine-terminated biomolecules and vice versa (76,80,142); (2) thiol (−SH) reactive maleimide coupling to cysteine and (sulfhydryl)-modified proteins and peptides; (3) avidin-biotin bridging (80,136,143); (4) metal-affinity driven self-assembly between polyhisitidine-appended biomolecules and metal-rich nanocrystals. This method relies on the affinity between polyhistidine tags and certain transition metal ions (eg, Ni and Zn) and requires direct interactions between the imidazole groups (on the tag) and the metal-rich surface of nanoparticles (83,144); (5) copper-catalyzed "Click" reaction, which requires access to biomolecules premodified with either alkynes or azides, together with azide- or alkyne-functionalized nanoparticles (133,145). Strain-promoted cyclooctyne-to-azide coupling does not require copper catalyst and is thus better suited for coupling onto QDs as Cu metal ions have been found to severely quench the QD PL (Fig. 6) (143,145). Aniline-catalyzed hydrazone ligation is an alternative strategy to the above list and has been applied by our group to couple QDs functionalized with aldehydes and the 2-hydrazinonicotinoyl (HYNIC) group attached to the target biomolecules, although no polymer functionalized nanocrystals were used; this reaction is efficient and can be monitored optically by tracking the absorption of the hydrazone chromophore at 354 nm (Fig. 6**C**) (146).

Use of Nanoparticles for Imaging. In this section, we will focus on a few representative examples where polymer-coated nanocrystals (QDs and magnetic nanoparticles) have been used for imaging and/or sensing purposes.

Magnetic Resonance Imaging. Magnetic nanoparticles have been intensively studied in the past decade for applications such as diagnostics and MRI (57,147,148). Often the nanoparticles either as of functionalized with antibodies are intravenously administered to an animal, and changes in the T2 MRI contrast signal is utilized to visualize the structure of the target lymph nodes, tissues, or

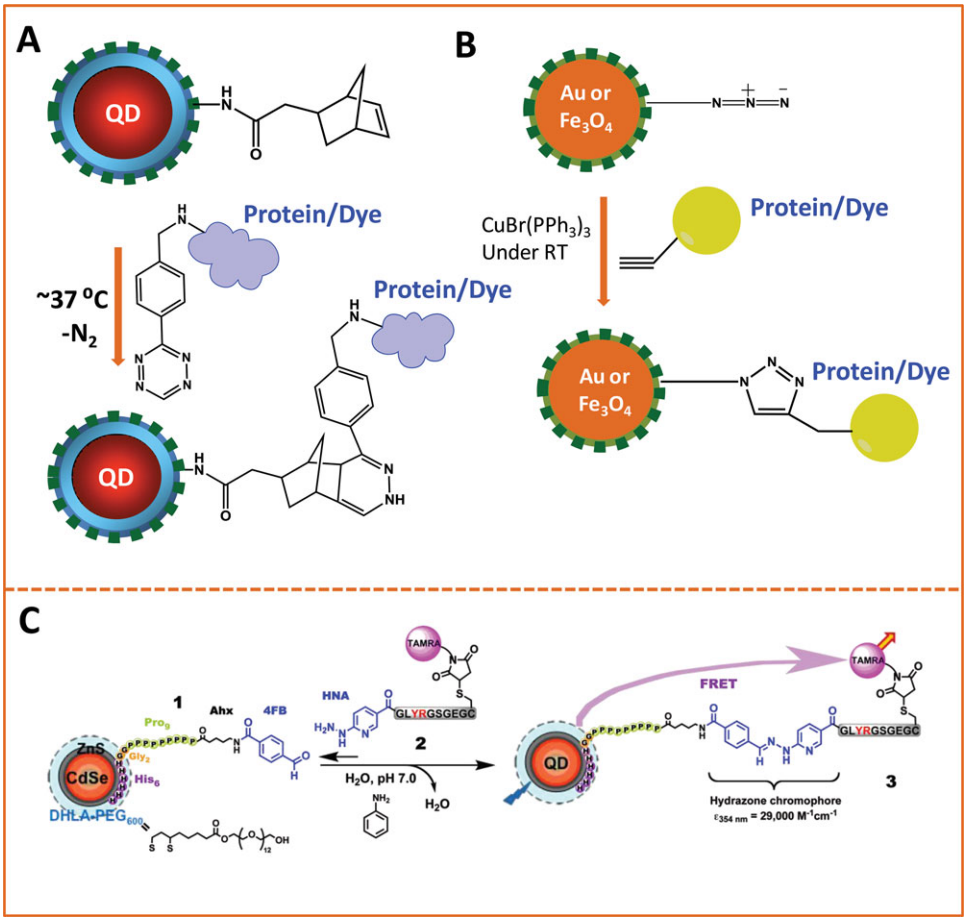

Fig. 6. (**A**) Schematics of the coupling strategy based on "Click" reaction between cyclooctyne and tetrazine moieties described in Ref. 145; (**B**) schematic representation of the copper-catalyzed cycloaddition reaction on AuNPs and iron oxide nanoparticles; (**C**) schematic representation of the aniline-catalyzed hydrazone ligation between 4-formylbenzoyl (an aldehyde) and HYNIC groups, as described in Ref. (146). Figures reproduced with permission from the American Chemical Society.

organs. For example, Hyeon and co-workers reported the use of versatile multiple-interaction ligands consisting of polydopamine and PEG functionalized iron oxide nanoparticles for time-dependent T2-weighted MRI study (Fig. 7) (141). The *in vivo* mouse imaging results obtained using these nanoparticles showed that the nanoparticles remained stable over extended blood circulation time. In addition, MTT assays showed that cell viability was not affected even following 24 and 72 h incubation with concentrations as high as 600 μg/mL of equivalent Fe.

Fluorescence Imaging. One of the most sought uses of inorganic nanocrystals in biology involves imaging and sensing. Indeed, QDs, AuNPs, and magnetic nanocrystals have large surfaces that can be functionalized with a

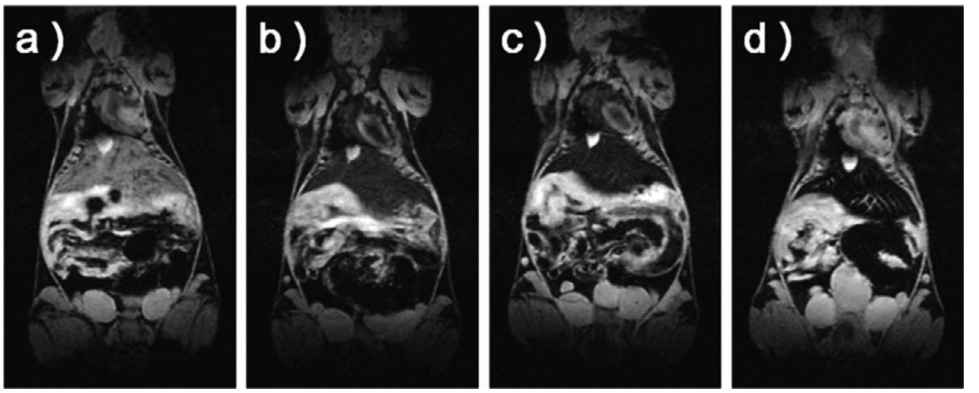

Fig. 7. Time-dependent T2-weighted MRI using a mouse model: (**a**) before, (**b**) immediately after, (**c**) 2 h after, and (**d**) 24 h after intravenous administration of multi-DOPA-functionalized magnetic nanoparticles as described in Ref. (141). Reproduced with permission from Wiley-VCH Verlag GmbH & Co. KGaA.

variety of hydrophilic and reactive ligands (1,12,13,15,147). Chemical tuning of their surface properties (eg, using a polymer coating) offers the unique ability to potentially control and affect their biodistribution through tuning of size and surface functionalities. For example, QDs exhibit several properties ideally suitable for use in live cell imaging, including resistance to chemical and photodegradation, narrow and tunable emission ranging from UV to near infrared (NIR), very high two-photon fluorescence signals, and the ability to excite any set of QDs far from their emission peak (97,149). Furthermore, *in vivo* visualization of tissue organs using NIR, for example, can provide real-time feedback during surgery or therapy. In some of the earlier studies, researchers focused on simple demonstrations to achieve long-term and multicolor imaging of some basic cellular processes along with multicolor labeling of fixed cells using QD-antibody conjugates (76,150,151). Other groups exploited the ability to self-assemble several copies of membrane surface receptors on a QD for efficient labeling of leukocytes and to probe membrane-specific processes such as T cell stimulation. Vascular transport of polymer-ligated QDs following intravenous injection was imaged through two-photon laser scanning microscopy, and time-dependent changes provided information about the kinetics of the QD distribution (Fig. 8) (81). Similarly, simple one-photon fluorescence using NIR-emitting QDs was used to carry out real-time mapping of sentinel lymph nodes in live animals (149,152). Several reviews have been published in the past few years detailing the effectiveness and limitations of such platforms for *in vivo* and *in vitro* imaging of cells and tissues.

Conclusions

We provided an overview of the strategies developed over the past decade for surface-functionalizing three representative inorganic nanocrystals, namely those made of Au, iron oxide, and luminescent QDs with amphiphilic polymers.

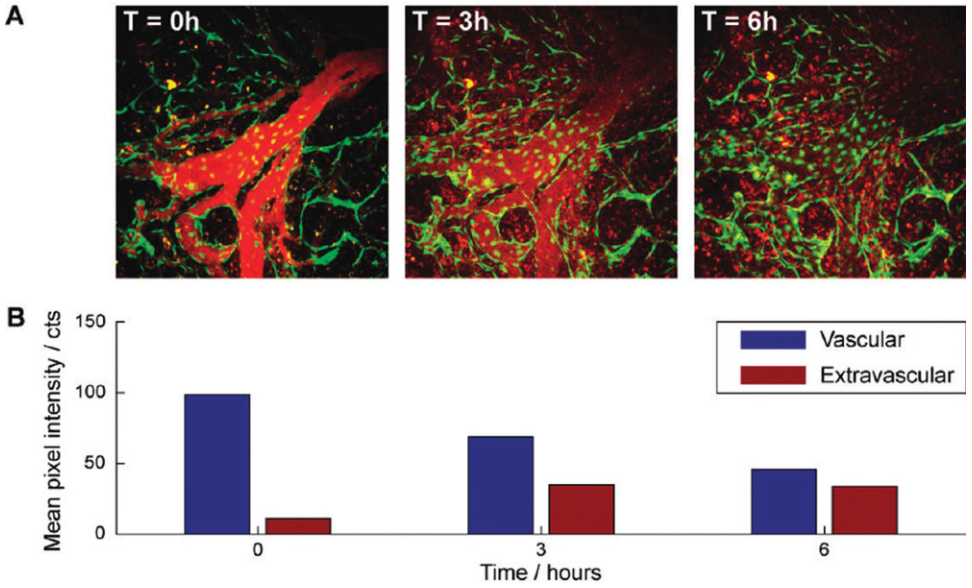

Fig. 8. (**A**) Fluorescence imaging of the blood vasculature in Tie2-GFP/FVB mice using red-emitting CdSe-CdS QDs capped with RAFT poly(PEG)PIL within the vessel lumen (at 0 and 3 h), or extravascular space in tumors (at 3 and 6 h). The green fluorescence originates from GFP in vascular endothelial cells that contour the vessel wall. (**B**) Time-dependent histogram showing the corresponding QD PL intensities within and outside the blood vessels. Reprinted from Ref. (81), with permission from the American Chemical Society.

Indeed, block copolymers with dimensions comparable to those of the nanocrystals, combined with the capacity to chemically tune their physical properties over multiple length scales, provide a great system for functionalizing various nanostructures and tune their solubility and functionalities. We described several examples where a variety of amphiphilic polymers have been used as capsules or/and ligands to promote the transfer of a diversity of inorganic nanomaterials (AuNPs, magnetic nanocrystals, and semiconductor QDs) to buffer media. In particular, we distinguished two sets of amphiphilic polymers (see Table 1). One set is made of block copolymers that present along with the hydrophilic block, a strongly hydrophobic block for tight interdigitation with the native ligands on the nanocrystals. The other set is made of polymers that contain anchoring groups that tightly ligate directly onto the inorganic surface of the nanoparticles by metal coordination. These materials usually present one or multiple anchoring groups that can competitively displace the native ligands on the nanocrystals, along with a hydrophilic block for water compatibility. Here, we described a variety of polymers with varying sizes, structures, and properties that can be used for either method: ligand exchange or encapsulation. We then concluded with a brief description of the commonly used conjugation strategies and applications in imaging based on either MRI or fluorescence detection.

BIBLIOGRAPHY

1. H. Mattoussi, G. Palui, and H. B. Na, *Adv. Drug. Deliv. Rev.* **64**, 138 (2012).
2. K. Saha, S. S. Agasti, C. Kim, X. N. Li, and V. M. Rotello, *Chem. Rev.* **112**, 2739 (2012).
3. M. H. M. Dias and P. C. Lauterbur, *Magnet Reson Med* **3**, 328 (1986).
4. P. T. Snee, R. C. Somers, G. Nair, J. P. Zimmer, M. G. Bawendi, and D. G. Nocera, *J. Am. Chem. Soc.* **128**, 13320 (2006).
5. X. Michalet, F. F. Pinaud, L. A. Bentolila, J. M. Tsay, S. Doose, J. J. Li, G. Sundaresan, A. M. Wu, S. S. Gambhir, and S. Weiss, *Science* **307**, 538 (2005).
6. A. M. Alkilany, S. E. Lohse, and C. J. Murphy, *Acc. Chem. Res.* 2012.
7. T. Hyeon, S. S. Lee, J. Park, Y. Chung, and H. B. Na, *J. Am. Chem. Soc.* **123**, 12798 (2001).
8. S. H. Choi, Bin H. Na, Y. I. Park, K. An, S. G. Kwon, Y. Jang, M. Park, J. Moon, J. S. Son, I. C. Song, W. K. Moon, and T. Hyeon, *J. Am. Chem. Soc.* **130**, 15573 (2008).
9. Y.-w. Jun, Y.-M. Huh, J.-s. Choi, J.-H. Lee, H.-T. Song, K. Kim, S. Yoon, K.-S. Kim, J.-S. Shin, J.-S. Suh, and J. Cheon, *J. Am. Chem. Soc.* **127**, 5732 (2005).
10. J. H. Lee, Y. M. Huh, Y. Jun, J. Seo, J. Jang, H. T. Song, S. Kim, E. J. Cho, H. G. Yoon, J. S. Suh, and J. Cheon, *Nat. Med.* **13**, 95 (2007).
11. H. Mattoussi and J. Cheon, *Inorganic Nanoprobes for Biological Sensing and Imaging*; Artech House: Boston, Mass., 2009.
12. I. L. Medintz, H. T. Uyeda, E. R. Goldman, and H. Mattoussi, *Nat. Mater.* **4**, 435–446 (2005).
13. P. Zrazhevskiy, M. Sena, and X. H. Gao, *Chem. Soc. Rev.* **39**, 4326 (2010).
14. M. De, P. S. Ghosh, and V. M. Rotello, *Adv. Mater.* **20**, 4225 (2008).
15. Y. C. Yeh, B. Creran, and V. M. Rotello, *Nanoscale* **4**, 1871 (2012).
16. A. L. Rogach, L. Katsikas, A. Kornowski, D. S. Su, A. Eychmuller, and H. Weller, *Ber. Bunsen-Ges. Phys. Chem.* **100**, 1772 (1996).
17. F. Aldeek, L. Balan, J. Lambert, and R. Schneider, *Nanotechnology* **19** (2008).
18. N. Gaponik, D. V. Talapin, A. L. Rogach, K. Hoppe, E. V. Shevchenko, A. Kornowski, A. Eychmüller, and H. Weller, *J. Phys. Chem. B* **106**, 7177 (2002).
19. C. B. Murray, D. J. Norris, and M. G. Bawendi, *J. Am. Chem. Soc.* **115**, 8706 (1993).
20. N. R. Jana and X. G. Peng, *J. Am. Chem. Soc.* **125**, 14280 (2003).
21. J. Park, K. J. An, Y. S. Hwang, J. G. Park, H. J. Noh, J. Y. Kim, J. H. Park, N. M. Hwang, and T. Hyeon, *Nat. Mater.* **3**, 891 (2004).
22. P. Reiss, M. Protiere, and L. Li, *Small* **5**, 154 (2009).
23. F. S. Bates and G. H. Fredrickson, *Phys. Today* **52**, 32 (1999).
24. N. Hadjichristidis, S. Pispas, and G. Floudas, *Block Copolymers: Synthetic Strategies, Physical Properties, and Applications*, John Wiley & Sons, Hoboken, N.J., 2003.
25. A. L. Efros, M. Rosen, M. Kuno, M. Nirmal, D. J. Norris, and M. Bawendi, *Phys. Rev. B* **54**, 4843 (1996).
26. D. J. Norris and M. G. Bawendi, *Phys. Rev. B* **53**, 16338 (1996).
27. D. J. Norris, A. L. Efros, M. Rosen and M. G. Bawendi, *Phys. Rev. B* **53**, 16347 (1996).
28. V. I. Klimov, *Nanocrystal Quantum Dots*, 2nd ed., CRC Press: Boca Raton, Fla., 2010.
29. A. L. Washington, M. E. Foley, S. Cheong, L. Quffa, C. J. Breshike, J. Watt, R. D. Tilley, and G. F. Strouse, *J. Am. Chem. Soc.* **134**, 17046 (2012).
30. J. H. Yu, S. H. Kwon, Z. Petrasek, O. K. Park, S. W. Jun, K. Shin, M. Choi, Il Y. Park, K. Park, Bin H. B. Na, N. Lee, D. W. Lee, J. H. Kim, P. Schwille, and T. Hyeon, *Nat. Mater.* **12**, 359 (2013).
31. J. H. Yu, X. Y. Liu, K. E. Kweon, J. Joo, J. Park, K. T. Ko, D. Lee, S. P. Shen, K. Tivakornsasithorn, J. S. Son, J. H. Park, Y. W. Kim, G. S. Hwang, M. Dobrowolska, J. K. Furdyna, and T. Hyeon, *Nat. Mater.* **9**, 47 (2010).

32. L. S. Li, J. T. Hu, W. D. Yang, and A. P. Alivisatos, *Nano Lett.* **1**, 349 (2001).
33. L. Manna, D. J. Milliron, A. Meisel, E. C. Scher, and A. P. Alivisatos, *Nat. Mater.* **2**, 382 (2003).
34. D. J. Milliron, S. Hughes, and A. P. Alivisatos, *Abstr. Pap. Am. Chem. Soc.* **227**, U274 (2004).
35. A. I. Ekimov and A. A. Onushchenko, *Sov. Phys. Semicond.* **16**, 775 (1982).
36. A. I. Ekimov and A. A. Onushchenko, *JETP Lett.* **34**, 345 (1981).
37. A. L. Efros and A. L. Efros, *Sov. Phys. Semicond.* **16**, 772 (1982).
38. N. F. Borrelli, D. W. Hall, H. J. Holland, and D. W. Smith, *J. Appl. Phys.* **61**, 5399 (1987).
39. D. W. Hall and N. F. Borrelli, *J. Opt. Soc. Am. B* **5**, 1650 (1988).
40. L. Brus, *J. Phys. Chem.* **90**, 2555 (1986).
41. A. Fojtik, H. Weller, U. Koch, and A. Henglein, *Ber. Bunsen-Ges. Phys. Chem.* **88**, 969 (1984).
42. H. Weller, U. Koch, M. Gutierrez, and A. Henglein, *Ber. Bunsen-Ges. Phys. Chem. Chem. Phys.* **88**, 649 (1984).
43. Z. A. Peng and X. G. Peng, *J. Am. Chem. Soc.* **123**, 183 (2001).
44. L. H. Qu, Z. A. Peng, and X. G. Peng, *Nano Lett.* **1**, 333 (2001).
45. M. V. Kovalenko, M. I. Bodnarchuk, J. Zaumseil, J. S. Lee, and D. V. Talapin, *J. Am. Chem. Soc.* **132**, 10085 (2010).
46. D. V. Talapin, A. L. Rogach, A. Kornowski, M. Haase, and H. Weller, *Nano Lett.* **1**, 207 (2001).
47. T. Pons, E. Pic, N. Lequeux, E. Cassette, L. Bezdetnaya, F. Guillemin, F. Marchal, and B. Dubertret, *ACS Nano* **4**, 2531 (2010).
48. B. O. Dabbousi, J. RodriguezViejo, F. V. Mikulec, J. R. Heine, H. Mattoussi, R. Ober, K. F. Jensen, and M. G. Bawendi, *J. Phys. Chem. B* **101**, 9463 (1997).
49. M. A. Hines and P. Guyot-Sionnest, *J. Phys. Chem. US* **100**, 468 (1996).
50. D. Thapa, V. R. Palkar, M. B. Kurup, and S. K. Malik, *Mater. Lett.* **58**, 2692 (2004).
51. A. N. Christensen, T. R. Jensen, C. R. H. Bahl, and E. DiMasi, *J. Solid State Chem.* **180**, 1431 (2007).
52. S. H. Tolbert, P. Sieger, G. D. Stucky, S. M. J. Aubin, C. C. Wu, and D. N. Hendrickson, *J. Am. Chem. Soc.* **119**, 8652 (1997).
53. S. H. Sun and C. B. Murray, *J. Appl. Phys.* **85**, 4325 (1999).
54. C. B. Murray, C. R. K., and M.G. Bawendi, *Ann. Rev. Mater. Sci.* **30**, 545 (2000).
55. F. X. Redl, C. T. Black, G. C. Papaefthymiou, R. L. Sandstrom, M. Yin, H. Zeng, C. B. Murray, and S. P. O'Brien, *J. Am. Chem. Soc.* **126**, 14583 (2004).
56. Y. W. Jun, Y. Y. Jung, and J. Cheon, *J. Am. Chem. Soc.* **124**, 615 (2002).
57. Y. W. Jun, J.-H. Lee, and J. Cheon, *Angew. Chem., Int. Ed.* **47**, 5122 (2008).
58. V. F. Puntes, K. M. Krishnan, and P. Alivisatos, *Appl. Phys. Lett.* **78**, 2187 (2001).
59. V. F. Puntes, P. Gorostiza, D. M. Aruguete, N. G. Bastus, and A. P. Alivisatos, *Nat. Mater.* **3**, 263 (2004).
60. Y. W. Jun, Y. M. Huh, J. S. Choi, J. H. Lee, H. T. Song, S. Kim, S. Yoon, K. S. Kim, J. S. Shin, J. S. Suh, and J. Cheon, *J. Am. Chem. Soc.* **127**, 5732 (2005).
61. J. R. Lai, K. V. P. M. Shafi, A. Ulman, K. Loos, N. L. Yang, M. H. Cui, T. Vogt, S. Estournes, and D. C. Locke, *J. Phys. Chem. B* **108**, 14876 (2004).
62. J. Turkevich, P. C. Stevenson, and J. Hillier, *Discuss. Faraday Soc.* 1951, 55.
63. G. Frens, *Nat. Phys. Sci.* **241**, 20 (1973).
64. M. Brust, M. Walker, D. Bethell, D. J. Schiffrin, and R. Whyman, *J. Chem. Soc., Chem. Commun.* 801 (1994).
65. E. Oh, K. Susumu, R. Goswami, and H. Mattoussi, *Langmuir* **26**, 7604 (2010).

66. F. Aldeek, M. A. Muhammed, G. Palui, N. Zhan, and H. Mattoussi, *ACS Nano* **7**, 2509 (2013).
67. X. P. Sun, S. J. Dong, and E. K. Wang, *Polymer* **45**, 2181 (2004).
68. A. Gole and C. J. Murphy, *Chem. Mater.* **17**, 1325 (2005).
69. A. Pucci, M. Bernabo, P. Elvati, L. I. Meza, F. Galembeck, C. A. D. Leite, N. Tirelli, and G. Ruggeri, *J. Mater. Chem.* **16**, 1058 (2006).
70. S. E. Lohse, J. R. Eller, S. T. Sivapalan, M. R. Plews, and C. J. Murphy, *ACS Nano* (2013).
71. X. Ye, L. Jin, H. Caglayan, J. Chen, G. Xing, C. Zheng, V. Doan-Nguyen, Y. Kang, N. Engheta, C. R. Kagan, and C. B. Murray, *ACS Nano* **6**, 2804 (2012).
72. T. K. Sau and C. J. Murphy, *J. Am. Chem. Soc.* **126**, 8648 (2004).
73. A. C. Templeton, M. P. Wuelfing, and R. W. Murray, *Acc. Chem. Res.* **33**, 27 (2000).
74. M. T. Fernández-Argüelles, A. Yakovlev, R. A. Sperling, C. Luccardini, S. Gaillard, S. A. Medel, J.-M. Mallet, J.-C. Brochon, A. Feltz, M. Oheim, and W. J. Parak, *Nano Lett.* **7**, 2613 (2007).
75. W. W. Yu, E. Chang, J. C. Falkner, J. Y. Zhang, A. M. Al-Somali, C. M. Sayes, J. Johns, R. Drezek, and V. L. Colvin, *J. Am. Chem. Soc.* **129**, 2871 (2007).
76. X. Y. Wu, H. J. Liu, J. Q. Liu, K. N. Haley, J. A. Treadway, J. P. Larson, N. F. Ge, F. Peale, and M. P. Bruchez, *Nat. Biotechnol.* **21**, 41 (2003).
77. T. Pellegrino, L. Manna, S. Kudera, T. Liedl, D. Koktysh, A. L. Rogach, S. Keller, J. Radler, G. Natile, and W. J. Parak, *Nano Lett.* **4**, 703 (2004).
78. W. C. W. Chan, S. M. Nie, *Science* **281**, 2016 (1998).
79. H. T. Uyeda, I. L. Medintz, J. K. Jaiswal, S. M. Simon, and H. Mattoussi, *J. Am. Chem. Soc.* **127**, 3870 (2005).
80. W. Liu, M. Howarth, A. B. Greytak, Y. Zheng, D. G. Nocera, A. Y. Ting, and M. G. Bawendi, *J. Am. Chem. Soc.* **130**, 1274 (2008).
81. W. H. Liu, A. B. Greytak, J. Lee, C. R. Wong, J. Park, L. F. Marshall, W. Jiang, P. N. Curtin, A. Y. Ting, D. G. Nocera, D. Fukumura, R. K. Jain, and M. G. Bawendi, *J. Am. Chem. Soc.* **132**, 472 (2010).
82. M. Bruchez, M. Moronne, P. Gin, S. Weiss, and A. P. Alivisatos, *Science* **281**, 2013 (1998).
83. H. Mattoussi, J. M. Mauro, E. R. Goldman, G. P. Anderson, V. C. Sundar, F. V. Mikulec, and M. G. Bawendi, *J. Am. Chem. Soc.* **122**, 12142 (2000).
84. A. N. Lukyanov and V. P. Torchilin, *Adv. Drug Deliv. Rev.* **56**, 1273 (2004).
85. Y. Kang and T. A. Taton, *Angew. Chem., Int. Ed.* **44**, 409 (2005).
86. Y. Chen, J. Cho, A. Young, and T. A. Taton, *Langmuir* **23**, 7491 (2007).
87. B. A. Kairdolf and S. Nie, *J. Am. Chem. Soc.* **133**, 7268 (2011).
88. D. H. Kim, A. Wei, and Y.-Y. Won, *ACS Appl. Mater. Interfaces* **4**, 1872 (2012).
89. K. S. Mayya, B. Schoeler, and F. Caruso, *Adv. Funct. Mater.* **13**, 183 (2003).
90. H.-C. Huang, S. Barua, D. B. Kay, and K. Rege, *CS Nano* **3**, 2941 (2009).
91. B. Ballou, B. C. Lagerholm, L. A. Ernst, M. P. Bruchez, and A. S. Waggoner, *Bioconjugate Chem.* **15**, 79 (2003).
92. X. H. Gao, Y. Y. Cui, R. M. Levenson, L. W. K. Chung, and S. M. Nie, *Nat. Biotechnol.* **22**, 969 (2004).
93. M. Zorn, W. K. Bae, J. Kwak, H. Lee, C. Lee, R. Zentel, and K. Char, *ACS Nano* **3**, 1063 (2009).
94. L. W. Liu, K. T. Yong, I. Roy, W. C. Law, L. Ye, J. W. Liu, J. Liu, R. Kumar, X. H. Zhang, and P. N. Prasad, *Theranostics* **2**, 705 (2012).
95. S. K. Chakraborty, J. A. J. Fitzpatrick, J. A. Phillippi, S. Andreko, A. S. Waggoner, M. P. Bruchez, and B. Ballou,*Nano Lett.* **7**, 2618 (2007).

96. B. C. Lagerholm, M. M. Wang, L. A. Ernst, D. H. Ly, H. J. Liu, M. P. Bruchez, and A. S. Waggoner, *Nano Lett.* **4**, 2019 (2004).
97. D. R. Larson, W. R. Zipfel, R. M. Williams, S. W. Clark, M. P. Bruchez, F. W. Wise, and W. W. Webb, *Science* **300**, 1434 (2003).
98. S. Courty, C. Luccardini, Y. Bellaiche, G. Cappello, and M. Dahan, *Nano Lett.* **6**, 1491 (2006).
99. M. Dahan, S. Levi, C. Luccardini, P. Rostaing, B. Riveau, and A. Triller, *Science* **302**, 442 (2003).
100. D. S. Lidke, P. Nagy, R. Heintzmann, D. J. Arndt-Jovin, J. N. Post, H. E. Grecco, E. A. Jares-Erijman, and T. M. Jovin, *Nat. Biotechnol.* **22**, 198 (2004).
101. M. J. Roberti, M. Morgan, G. Menendez, L. I. Pietrasanta, T. M. Jovin, and E. A. Jares-Erijman, *J. Am. Chem. Soc.* **131**, 8102 (2009).
102. E. E. Lees, T.-L. Nguyen, A. H. A. Clayton, and P. Mulvaney, *ACS Nano* **3**, 1121 (2009).
103. J. C. Jewett and C. R. Bertozzi, *Chem. Soc. Rev.* **39**, 1272 (2010).
104. C. Schieber, A. Bestetti, J. P. Lim, A. D. Ryan, T.-L. Nguyen, R. Eldridge, A. R. White, P. A. Gleeson, P. S. Donnelly, S. J. Williams, and P. Mulvaney, *Angew. Chem., Int. Ed.* **51**, 10523 (2012).
105. X. S. Wang, T. E. Dykstra, M. R. Salvador, I. Manners, G. D. Scholes, and M. A. Winnik, *J. Am. Chem. Soc.* **126**, 7784 (2004).
106. M. F. Wang, M. Zhang, J. Li, S. Kumar, G. C. Walker, G. D. Scholes, and M. A. Winnik, *ACS Appl. Mater. Interfaces* **2**, 3160 (2010).
107. M. F. Wang, N. Felorzabihi, G. Guerin, J. C. Haley, G. D. Scholes, and M. A. Winnik, *Macromolecules* **40**, 6377 (2007).
108. T. Jin, F. Fujii, E. Yamada, Y. Nodasaka, and M. Kinjo, *J. Am. Chem. Soc.* **128**, 9288 (2006).
109. E. Pöselt, C. Schmidtke, S. Fischer, K. Peldschus, J. Salamon, H. Kloust, H. Tran, A. Pietsch, M. Heine, G. Adam, U. Schumacher, C. Wagener, S. Förster, and H. Weller, *ACS Nano* **6**, 3346 (2012).
110. H. Kloust, E. Pöselt, S. Kappen, C. Schmidtke, A. Kornowski, W. Pauer, H.-U. Moritz, and H. Weller, *Langmuir* **28**, 7276 (2012).
111. E. Poselt, S. Fischer, S. Foerster, and H. Weller, *Langmuir* **25**, 13906 (2009).
112. H. Kloust, C. Schmidtke, A. Feld, T. Schotten, R. Eggers, U. E. A. Fittschen, F. Schulz, E. Pöselt, J. Ostermann, N. G. Bastús, and H. Weller, *Langmuir* **29**, 4915 (2013).
113. X. Zhang, M. R. Servos, and J. Liu, *J. Am. Chem. Soc.* **134**, 7266 (2012).
114. R. Levy, N. T. K. Thanh, R. C. Doty, I. Hussain, R. J. Nichols, D. J. Schiffrin, M. Brust, and D. G. Fernig, *J. Am. Chem. Soc.* **126**, 10076 (2004).
115. M. C. Daniel and D. Astruc, *Chem. Rev.* **104**, 293 (2004).
116. P. Dash and R. W. J. Scott, *Chem. Commun.* 812 (2009).
117. J. M. Kogot, H. J. England, G. F. Strouse, and T. M. Logan, *J. Am. Chem. Soc.* 2008, **130**, 16156.
118. K. E. Sapsford, W. R. Algar, L. Berti, K. B. Gemmill, B. J. Casey, E. Oh, M. H. Stewart, and I. L. Medintz, *Chem. Rev.* **113**, 1904 (2013).
119. H. Hakkinen, *Nat. Chem.* **4**, 443 (2012).
120. K. O. Aruda, M. Tagliazucchi, C. M. Sweeney, D. C. Hannah, G. C. Schatz, and E. A. Weiss, *Proc. Natl. Acad. Sci. U. S. A.* **110**, 4212 (2013).
121. P. D. Jadzinsky, G. Calero, C. J. Ackerson, D. A. Bushnell, and R. D. Kornberg, *Science* **318**, 430 (2007).
122. J. R. Reimers, Y. Wang, B. O. Cankurtaran, and M. J. Ford, *J. Am. Chem. Soc.* **132**, 8378 (2010).

123. G. P. Mitchell, C. A. Mirkin, and R. L. Letsinger, *J. Am. Chem. Soc.* **121**, 8122 (1999).
124. J. S. Kang, and T. A. Taton, *Langmuir* **28**, 16751 (2012).
125. L. Liu, X. Guo, Y. Li, and X. Zhong, *Inorg. Chem.* **49**, 3768 (2010).
126. I. Yildiz, E. Deniz, B. McCaughan, S. F. Cruickshank, J. F. Callan, and F. i. M. Raymo, *Langmuir* **26**, 11503 (2010).
127. I. Yildiz, B. McCaughan, S. F. Cruickshank, J. F. Callan, and F. I. M. Raymo, *Langmuir* **25**, 7090 (2009).
128. G. Palui, H. B. Na, and H. Mattoussi, *Langmuir* **28**, 2761 (2012).
129. E. Giovanelli, E. Muro, G. Sitbon, M. Hanafi, T. Pons, B. Dubertret, and N. Lequeux, *Langmuir* **28**, 15177 (2012).
130. X. Chen, J. Lawrence, S. Parelkar, and T. Emrick, *Macromolecules* **46**, 119 (2012).
131. K. E. Sapsford, T. Pons, I. L. Medintz, S. Higashiya, F. M. Brunel, P. E. Dawson, and H. Mattoussi, *J. Phys. Chem. C* **111**, 11528 (2007).
132. H.-S. Han, J. D. Martin, J. Lee, D. K. Harris, D. Fukumura, R. K. Jain, and M. Bawendi, *Angew. Chem., Int, Ed,* **52**, 1414 (2013).
133. P. Zhang, S. Liu, D. Gao, D. Hu, P. Gong, Z. Sheng, J. Deng, Y. Ma, and L. Cai, *J. Am. Chem. Soc.* **134**, 8388 (2012).
134. Y. Sahoo, H. Pizem, T. Fried, D. Golodnitsky, L. Burstein, C. N. Sukenik, and G. Markovich, *Langmuir* **17**, 7907 (2001).
135. S.-W. Kim, S. Kim, J. B. Tracy, A. Jasanoff, and M. G. Bawendi, *J. Am. Chem. Soc.* **127**, 4556 (2005).
136. H. Wei, N. Insin, J. Lee, H.-S. Han, J. M. Cordero, W. Liu, and M. G. Bawendi, *Nano Lett.* **12**, 22 (2011).
137. L. Sandiford, A. Phinikaridou, A. Protti, L. K. Meszaros, X. Cui, Y. Yan, G. Frodsham, P. A. Williamson, N. Gaddum, R. M. Botnar, P. J. Blower, M. A. Green, and R. T. M. de Rosales, *ACS Nano* **7**, 500 (2012).
138. C. Xu, K. Xu, H. Gu, R. Zheng, H. Liu, X. Zhang, Z. Guo, and B. Xu, *J. Am. Chem. Soc.* **126**, 9938 (2004).
139. E. Amstad, T. Gillich, I. Bilecka, M. Textor, and E. Reimhult, *Nano Lett.* **9**, 4042 (2009).
140. H. Bin Na, G. Palui, J. T. Rosenberg, X. Ji, S. C. Grant, and H. Mattoussi, *ACS Nano* **6**, 389 (2012).
141. D. Ling, W. Park, Y. I. Park, N. Lee, F. Li, C. Song, S.-G.Yang, S. H. Choi, K. Na, and T. Hyeon, *Angew. Chem., Int. Ed.* **50**, 11360 (2011).
142. K. Susumu, H. T. Uyeda, I. L. Medintz, T. Pons, J. B. Delehanty, and H. Mattoussi, *J. Am. Chem. Soc.* **129**, 13987 (2007).
143. W. Liu, A. B. Greytak, J. Lee, C. R. Wong, J. Park, L. F. Marshall, W. Jiang, P. N. Curtin, A. Y. Ting, D. G. Nocera, D. Fukumura, R. K. Jain, and M. G. Bawendi, *J. Am. Chem. Soc.* **132**, 472 (2009).
144. K. Susumu, I. L. Medintz, J. B. Delehanty, K. Boeneman, and H. Mattoussi, *J. Phys. Chem. C* **114**, 13526 (2010).
145. H.-S. Han, N. K. Devaraj, J. Lee, S. A. Hilderbrand, R. Weissleder, and M. G. Bawendi, *J. Am. Chem. Soc.* **132**, 7838 (2010).
146. J. B. Blanco-Canosa, I. L. Medintz, D. Farrell, H. Mattoussi, and P. E. Dawson, *J. Am. Chem. Soc.* **132**, 10027 (2010).
147. J. Cheon and J.-H. Lee, *Acc. Chem. Res.* **41**, 1630 (2008).
148. N. Lee and T. Hyeon, *Chem. Soc. Rev* **41**, 2575 (2012).
149. S. Kim, Y. Lim, E. Soltesz, A. De Grand, J. Lee, A. Nakayama, J. Parker, T. Mihaljevic, R. Laurence, D. Dor, L. Cohn, M. Bawendi, and J. Frangioni, *Nat. Biotechnol.* **22**, 93 (2004).

150. J. K. Jaiswal, H. Mattoussi, J. M. Mauro, and S. M. Simon, *Nat. Biotechnol.* **21**, 47 (2003).
151. B. Dubertret, P. Skourides, D. J. Norris, V. Noireaux, A. H. Brivanlou, and A. Libchaber, *Science* **298**, 1759 (2002).
152. T. Pons, E. Pic, N. Lequeux, E. Cassette, L. Bezdetnaya, F. Guillemin, F. Marchal, and B. Dubertret, *ACS Nano* **4**, 2531 (2010).

GOUTAM PALUI
WENTAO WANG
FADI ALDEEK
HEDI MATTOUSSI
Florida State University
Tallahassee, Florida